



FINAL REPORT

IN SITU COMPARISON BETWEEN DIRECT
AND MAGNETIZATION CRITICAL CURRENT
MEASUREMENTS IN REBCO COATED
CONDUCTORS

Alexander Stangl
1020 Wien

Scholarship
01/07/2013 - 07/06/2013
National High Magnetic Field Laboratories, Florida State University



TECHNISCHE
UNIVERSITÄT
WIEN
Vienna University of Technology



1 Abstract

High temperature superconductors in the form of coated conductors, made from $\text{REBa}_2\text{Cu}_3\text{O}_{7-x}$ (RE = rare earth element) are playing an increasing role in the fabrication of magnets and the development of high current and high field applications. For those purposes high critical current densities J_c and good magnetic properties homogeneous over the full length (hundreds of meters) of the tape are necessary.

This report presents results of in situ magnetization and I_c reel to reel measurements in several tapes of REBCO coated conductors from Superpower Inc. with lengths more than 100 m. Reel to reel measurements enable continuous critical current $I_c(x, B, \theta)$ evaluations of superconducting tapes for commercial available lengths of superconducting tape with very high resolution. Further, an array of Hall probes was installed for magnetization measurements and contact free observation of the current flow, which provide a reliable and very fast, but non-calibration free opportunity for the analysis of long tapes. We made detailed comparisons of those two methods. Our results confirm the validity of the magnetization method to find inhomogeneities. The possibility of identifying defects in tapes is crucial for the construction of magnets, since a single defect degrades the performance of the whole magnet.

Up to now these non-destructive measurements were made at liquid nitrogen temperature. We developed a measurement setup for reel-to-reel Hall probe measurements at liquid helium temperature. Such measurements are unique at present. This temperature range is interesting, because the construction of all superconducting magnets for generating fields above 30 T requires cooling to 4.2 K. While coated conductors are widely characterized at 77 K, the flux pinning mechanisms are poorly known at temperatures below $T_c/2$. The mechanisms may be very different at high and low temperatures. Because of the strong reduction of thermal fluctuation effects weaker flux pins are becoming more important.

I'd like to thank Jan J. Jaroszynski, John Sinclair, Michael Santos, Xinbo Hu, David C. Larbalestier and Harald W. Weber for the good collaboration.

Contents

1	Abstract	2
2	Introduction and Motivation	4
2.1	Superconductivity	5
2.2	Bean's Critical State Model	6
3	Hall probe measurements	7
3.1	Theory of Operation	7
3.1.1	Calibration	7
4	YatesStar	9
4.0.2	I_c and n -values	9
4.1	YatesStar 1.1	10
4.1.1	Position Calculation and Velocity Correction	10
4.1.2	Extension for Helium Measurements	11
4.2	Data Evaluation	11
4.2.1	Position Determination	11
4.2.2	Assessment of I_c	11
4.2.3	Evaluation of j_c	12
4.2.4	Evaluation of I_c	12
5	Results	13
5.1	M3-747	13
5.2	M4-52	13
5.3	M3-998 Insulated Tape	15
5.4	SP57	19
5.5	SP59	19
5.6	Tape Collection (SP60-SP64)	21
5.7	SP41	22
6	Conclusions	24
	Bibliography	25

2 Introduction and Motivation

The present work is concerned with the analysis of long superconducting $\text{YBa}_2\text{Cu}_3\text{O}_{7-x}$ tapes. The motivation of this work is the use of these high temperature superconductors (HTS) in several applications, especially the 32 T all superconducting magnet project at the National High Magnetic Field Laboratory (NHMFL). For those purposes high critical current densities J_c and good magnetic properties homogeneous over long lengths are necessary.

In this work we upgraded an apparatus, YatesStar [5, 6, 15], for simultaneous magnetization and I_c reel-to-reel measurements of REBCO tapes with lengths of more than 100 m at liquid nitrogen temperature and developed the possibility of - at present - unique continuous magnetization measurements at liquid helium temperature.

Although superconductivity is known for more than 100 years and alloys with transition temperatures above the boiling temperature of liquid nitrogen were discovered 25 years ago, superconductivity is still in the interest of research groups all over the world to understand the fundamental physics of especially type II superconductors and to use the benefits and attractive perspectives for applications. At the moment a 32 T all superconducting magnet is developed at the NHMFL, by combining outer coils made of low temperature superconductors (LTS) and inner coils out of high temperature superconductors. The use of YBCO coated conductors (CC) as HTS material provides an increase in central field and a large reduction of operation costs compared to resistive magnets [14]: the normal Keck magnet at the NHMFL at 15 T consumes 6.8 MW, a superconducting magnet with the same field less than 1 kW. Further superconducting magnets have much better homogeneity, which is very important to magnetic resonance measurements and can be built more compact, due to the capacity of carrying higher currents.

There is one commercial quality inspection tool for superconducting tapes, TapeStar from THEVA GmbH and several scientific projects of long tape analysis, all based on magnetization measurements with Hall probes at 77 K [7, 8, 10, 13]. The innovation of our work is the comparison of transport current I_c measurements and magnetization measurements over the full length of superconducting tapes at 77 K and the latter as well at 4.2 K. Transport current measurements need several contacts (at least two voltage and two current contacts) which could damage the tape by friction or too high currents and continuous measurements are not possible, since the current must be ramped to determine the critical current defined by a certain field criterion. During this process, which has a finite duration, the tape can not be moved. To avoid noise produced by the motion of the tape, current sweeps, local changes of the field, thermal heating and others, a pause before each local I_c measurement is reasonable, which extends the time of the analysis. In comparison Hall probe measurements are fast, contact-free and thereby non-destructive with high spatial resolution. On the other hand they are susceptible to

various influences and non-calibration free. The possibility to use both methods at the same time, or rather in situ one after the other, allows us to test and confirm the validity of magnetization measurements to assess the local critical currents and find interference factors to further improve the tape analysis using Hall probes. Since magnet bores with cryostats are limited to a few centimeters, a very compact measuring setup is essential for low temperature measurements. Transport measurements in this temperature range would need thick current leads to carry high currents without Joule heating. These requirements are hardly compatible with the given space in the bore. Therefore Hall probe measurements are a promising candidate for this very low temperature range.

Previously it was shown for short samples [11], that efforts to optimize the conductor production for high temperature applications lead to an increasing I_c at 77 K but worsen at the same time in-field properties at liquid helium temperature. Intensive studies of pinning mechanisms, especially introduced by BaZrO₃ nanorods at the Applied Superconductivity Center [3, 11, 16] have shown there is no a priori known correlation between 77 K and 4.2 K. There might be different flux pinning mechanisms due to smaller vortex core sizes and the deduction of thermal fluctuation at low temperatures, which allow weaker pins to become more important. These results make the characterization of CCs at low temperatures essential for their use in low temperature applications.

Summing up the aim of this work is to develop fast and non-destructive magnetization measurements, proof their validity in comparison with local transport measurements over long lengths at liquid nitrogen temperature and based on these results built a prototype for reel-to-reel magnetizations measurements at 4.2 K.

2.1 Superconductivity

Superconductivity is a state which occurs at low temperatures with extraordinary electrical properties. Superconductors lose electric resistance below a certain material depended temperature, the critical temperature T_c . This property is limited by a critical current density J_c , an external critical field and as well the temperature T_c . Zero resistance is essential but not sufficient to make superconductivity a thermodynamic phase. Only in combination with the ejection of weak external magnetic fields the requirements are full-filled. This second very important characteristic of superconductivity is called Meißner effect. The limiting field for type-I SC is the thermodynamical critical field B_c which is defined by the difference in the Gibbs free energy G of the normal and superconducting state

$$E_c = G_n(0, T) - G_s(0, T) = \frac{\mu_0 H_c^2(T)}{2} V, \quad (2.1)$$

with V as volume of the sample and μ_0 as the vacuum permeability. This energy difference is due to the condensation of electron pairs with reverse wave vectors and spins in to Cooper pairs caused by a small attraction between electrons.



Figure 2.1: The local fields inside the superconductor for (a) increasing and (b) decreasing external fields described by the Bean model [2]

2.2 Bean's Critical State Model

There are two different kinds of superconductivity, determined by their behavior in external magnetic fields. Type-I superconductivity only exists below the critical field B_c . If an external magnetic field exceeds this critical field all superconductivity is lost. For type-II superconductors two critical fields, the lower B_{c1} and upper B_{c2} are necessary to describe its response to magnetic fields. Below B_{c1} type-II superconductors expel the field (Meißner phase). In a field range between B_{c1} and B_{c2} superconductivity still exists, but quantized flux lines penetrate the interior of the superconductor. Due to this penetration type-II superconductors show an irreversible magnetization if there is an applied field higher than B_{c1} . After intensive studies of magnetization curves of hard superconductors Bean [1, 2] published his theory of the magnetization and hysteresis of high-field superconductors. Under the premise that a limiting macroscopic superconducting current density exists, he assumed that fields smaller than $\mu_0 H_{c1}$ are screened by screening currents flowing only at the surface. Further fields $\mu_0 H$, $H_{c1} < H < H_{c2}$, are shielded by local currents flowing in layers to the full amount of the critical current density. Hence, the sample carries a maximum supercurrent. In his first approximation the current density is field independent ($J_c(B) = \text{const.}$). This treatment is appropriate as long as the applied field is much less than the critical field, especially since the difference $H_a - H^*$ is relevant. Kim et al. [12] introduced an inversely proportional relation for the field dependence of the current density. There are several relations in literature to describe J_c as a function of magnetic field in different regions of the field.

The process of magnetization can be described by steps as shown in fig. 2.1 for an ideal infinite cylinder with diameter D . Increasing the applied field from $H = 0$ (more precise from $H = H_{c1}$, but H_{c1} is very small) to $H = H^*$ quantized magnetic flux penetrates the outer layers of the superconductor. Due to this gradient of flux lines a current is flowing locally. With a constant current density the decrease of the field is linear, as predicted by Ampère's law. The penetration depth is therefore field dependent. At an applied field of $H = H^*$ the whole sample is penetrated by field and the current density is non-zero anywhere in the sample. Further increasing fields can not be shielded more efficiently. In this simple model $H(r = 0) = H(r = \frac{D}{2}) - H^*$ describes the field in the center of the sample, if the applied field H exceeded H^* . Fig. 2.1 (b) shows the remanent magnetization after a field H_0 has been applied and removed. If the applied field $H \geq 2H^*$ the remanent magnetization in the center of the field reaches its maximum.

3 Hall probe measurements

With the goal to show the possibilities of Hall probe (HP) measurements, we built several sensor heads with three and four Hall probes. Later we produced an array with seven HPs as well. We used transverse Hall generators 2101-100 from Lake Shore. The HPs are glued with GE Varnish to the surface of sample holder adapters with 16 connections. Thus we are able to easily exchange the HP arrays. The HPs are connected in serial to ensure the same driving current through all HPs and they are mounted with same alignment.

3.1 Theory of Operation

The measurement of magnetic field with Hall probes is based on the eponymous Hall Effect. In 1879 Hall [9] investigated the influence of a magnetic field on the current in a conductor. Predicted by the Lorentz force

$$\vec{F}_L = q(\vec{E} + \vec{v} \times \vec{B}) \quad (3.1)$$

a point charge q with velocity \vec{v} experiences a force in an external magnetic field \vec{B} . Due to a different sign, electrical positive and negative charges will be separated inside the current leading conductor. An excess charge on one side creates a transverse electric field which pushes the electrons in the opposite direction. At equilibrium this potential difference can be measured. Hall probe materials are mostly semiconductors from columns III and V of the periodic chart, which provide a high charge mobility. The Hall voltage is proportional to the magnetic field B and given by the relation

$$U_H = A_H IB, \quad (3.2)$$

with the driving current I through the conductor and a material and thickness depending Hall coefficient.

3.1.1 Calibration

According to equation 3.2 the transverse voltage over the Hall probe should vanish in zero field. In practice Hall probes show an offset. A calibration determines the offset and the Hall coefficient A_H .

To do so, we placed a Hall probe array in the center of a 1 T electromagnet and orientated it in the field. The applied field was measured by an installed and already calibrated Hall probe. At a given field we measured the voltage over a certain time and averaged the values. Especially in low fields the offset U_0 is very important for the

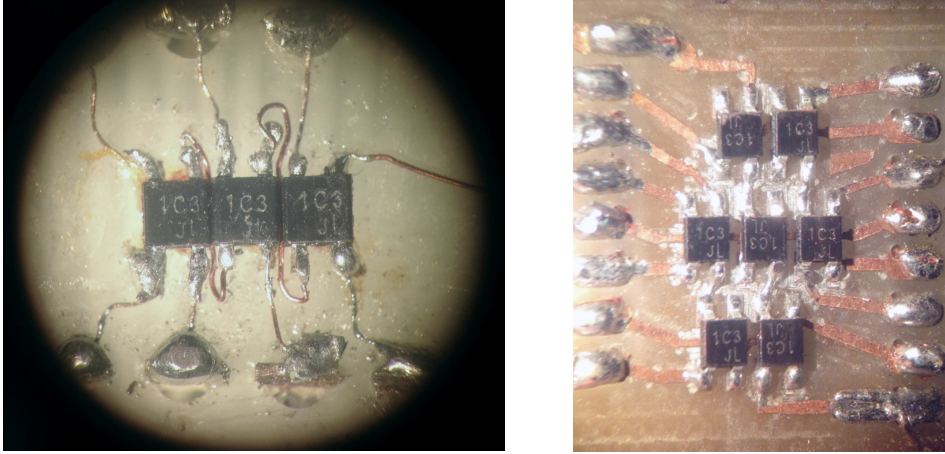


Figure 3.1: Hall probe sensor heads with (a) three Hall probes mounted close to each other for tape measurements and (b) with seven Hall probes; the first line is shifted by 1.6 mm and the third by 0.8 mm from the left side to the second line

determination of the Hall coefficient A_H . If the voltage is non-vanishing, U_H/B goes to plus or minus infinity. A good correction leads to a satisfying linearity for the Hall coefficient up to 400 mT, which is sufficient for our initial measurements. A_H results in $228 \text{ VA}^{-1}\text{T}^{-1}$. With a control current of $100 \mu\text{A}$ the magnetic sensitivity is $22.8 \mu\text{VmT}^{-1}$. This high sensitivity allows us to measure tenths to hundredths of a millitesla.

The array in figure 3.1 (a) was used for early magnetization measurements. The Hall probes are glued as close as possible and the current contacts are connected in serial.. The length of each HP is 1.5 mm. The active area of the Hall probe is very good in the center. Therefore, with three Hall probes as shown, a width of $\approx 3 \text{ mm}$ is covered.

For more detailed observations a higher Hall probe density is necessary. An arrangement of seven Hall probes, each shifted by a third of its length to the vertical position of the previous allows us to measure with a higher spatial resolution and to evaluate critical parameters. This array was fabricated by the electronic shop of the NHMFL. The sensor is shown in figure 3.1 (b). The distance between the Hall generators in one line is 0.3 mm, respectively. Therefore a width of 3.6 mm is covered by seven HPs and the resolution over the tape width is 0.6 mm.

4 YatesStar

YatesStar (YS*) is an apparatus, developed by J. Yates Coulter [5, 6, 15] at the Superconductivity Technology Center at Los Alamos National Laboratory to make critical current measurements of long tapes at 77 K. The tape unwinds from a feed reel and gets wound on the take-up reel, controlled by two motors. In between two silver pulleys support the tape transport and serve as current leader for the transport current measurements. On the axis of these pulleys external encoders record the tape position. YatesStar is shown in 4.1 (a) and a schematic diagram of its method of operation in 4.1 (b).

Due to the decreasing radius of the tape on the feed reel during the measurement the velocity of the tape decreases as well, since the velocity of the motor is constant. A missing regulation leads to an increasing resolution in length during the measurement, and therefore a longer measurement duration.

In between the current pulleys two rotating permanent magnets with a maximum field of ≈ 0.53 T and a DC electromagnet are mounted. The field of the electromagnet can be adjusted over a current source and is usually set to a field of the same amount as the permanent magnets to produce same conditions for the measurements. Its field is parallel to the *c*-axis of the superconducting tape. The permanent magnets can be rotated so that the field lies in the *ab* plane or is parallel to the *c*-axis of the conductor. The tape is moved through the center of the field of the magnet arrangements. The voltage tabs are located in front and behind the magnets, respectively. Usually the distance between the voltage tabs is important for measuring the I_c using the usual $1 \mu\text{V}/\text{cm}^{-1}$ criterion. In this case the applied magnetic fields reduce the I_c and the voltage drops outside the field maxima are negligible. The length of good homogeneity of the fields is about 2 cm each and is used for the calculation of the I_c . Three small pulleys ensure an electrical contact between the tape and the voltage tabs. These in-field measurements not only allow measurements with weaker transport currents, but also prevent tape damage between the current leads and the outer voltage tabs, since the critical current density outside the field is higher. Damages worsen the I_c , but only major defects lower the critical current as far as the field does.

During the measurement YatesStar is situated in a bath of liquid nitrogen. Since measurements with a very high resolution up to 2 cm and a total tape length of more than 100 m could take up to two days, a good thermal insulation is sufficient. Improvements increased the time between nitrogen refills substantially to 6-8 hours.

4.0.2 I_c and n -values

YatesStar automatically calculates two important parameters for the analysis of superconductors, $I_c(x)$ and the parameter $n(x)$ from a power law $V \propto I^n$ for a certain position

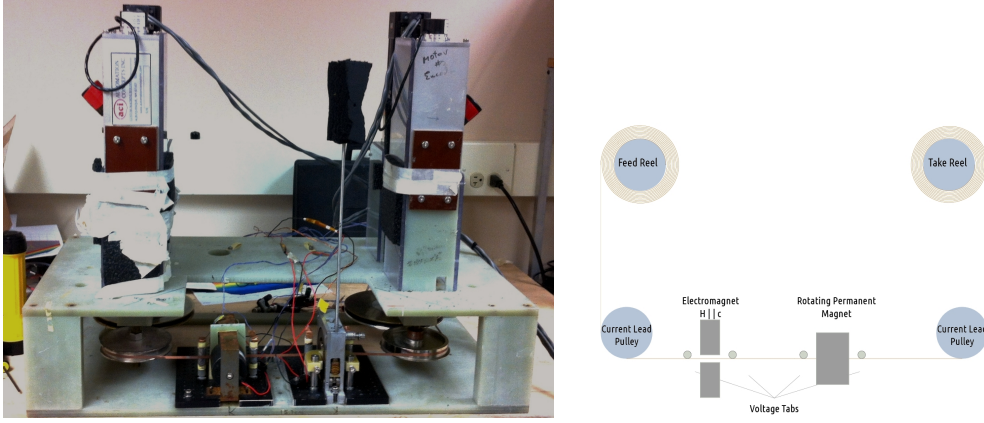


Figure 4.1: (a) YatesStar, (b) schematic diagram of reel-to-reel 4-probe transport current measurement setup

x . $I_c(x)$ depends on the local critical current density $j_c(x)$ and the superconducting cross section $A(x)$. However, n only depends on j_c . Therefore it is possible to distinguish between local variations in the cross section or in j_c [6]. The critical current density depends on the microstructure of the CC.

4.1 YatesStar 1.1

In the following there is a discussion of new developments for the magnetization measurements.

A simple construction was built to mount the Hall probes. Vertical up and down motion of the tape can modify the measured signal very strongly. A tape stabilizer was developed to suppress those fluctuations in tape high.

4.1.1 Position Calculation and Velocity Correction

The velocity of the tape is defined by the velocity of the feed motor and the current radius of the tape on the spool. The decreasing radius leads to a decrease in the velocity of the tape. Since we are using two different systems to control the motors and measure the voltage of the Hall probes over time we have to recalculate the time depending position. A simplified model gives the position after i revolution of the motor:

$$P_i = P_0 + 2\pi ir - \pi \frac{(i^2 - i)}{2} dr, \quad (4.1)$$

with the initial outer radius r and the thickness of the tape dr . i is known and r and dr can be measured by ruler or can be fitted to position data from the system which controls the motors. The thickness of the tapes is in the order of 0.1 mm.

4.1.2 Extension for Helium Measurements

Helium is rare on earth and the price for liquid helium is much higher than for liquid nitrogen. For continuous tape measurements at 4.2 K we had to fit our measuring equipment into a 52 mm wide bore of a cryostat. Transport current measurements are not compatible with such conditions, but magnetization measurements are a promising candidate. We developed an extension for reel-to-reel magnetization measurements inside a magnet bore. Therefore YS* is mounted on the top of a cryostat and the tape is transported into the bore, guided by several small pulleys. An outer magnet produces a vertical field inside the bore. In the center of the magnet, where the field has its maximum the tape turns up again and gets magnetized. Above the magnet but still in the cryostat we measure the remanent field of the tape.

4.2 Data Evaluation

The Hall probe measurements provide the magnetic field in a finite distance of the surface of the superconductor. Obvious defects can be seen in a two dimensional field map. There are several methods to calculate the critical parameters of the tape, described below. The field in the center of the tape is symmetrically influenced by all currents flowing across the tape width. Any inhomogeneities in the critical current density j_c in z direction affect the measured field in the center [17]. Therefore the field distribution along the tape length in the center of the sample is proportional to the critical current I_c as shown later.

4.2.1 Position Determination

In the early measurements we were not able to record the position for the Hall scans. To compare the data of the transport current ($I_c(x)$) and the magnetization ($U_H(t)$) measurement we first have to determinate $x(t)$ with equation 4.1 to get $U_H(x(t))$.

Temporarily we measured the position and the Hall voltage with different measuring rates. The total number of measured position points is p , the number of voltage points is q . Since the ratio $p/q \approx 1$, a linear interpolation gives a sufficient good result for providing q position points.

A software solution based on LabVIEW which controls the motors and reads the voltmeter is still under development.

4.2.2 Assessment of I_c

One widely used method to assess the critical current is to calibrate the Hall probe system. A calibration factor c (A/mT) is determined, which links the Hall voltage signal to the critical current with the linear relation $I_c = c \cdot B$. Since we are measuring the local $I_c(x)$ over the full length of the tape, we are able to calibrate the Hall measurement without cutting a short sample from the end.

4.2.3 Evaluation of j_c

According to Bean's critical state model j_c corresponds to the slope of the magnetization in z direction. Although Brandt and Indenbom [4] showed that this assumptions are not valid for flat superconductors in a perpendicular field due to demagnetization effects, the application of this model should provide the order of magnitude. The slope m can be calculated by a linear regression of the field profile

$$m = \frac{n \sum_{i=1}^n (z_i \cdot B(x, y, z_i)) - \sum_{i=1}^n z_i \sum_{i=1}^n B(x, y, z_i)}{n \sum_{i=1}^n (z_i^2) - (\sum_{i=1}^n z_i)^2}, \quad (4.2)$$

with z_i as the vertical position of the Hall probe i , y the distance between the sensors and tape surface, $B(x, y, z_i)$ the field at the position (x, y, z_i) and n is the number of Hall probes, which are used for the regression.

4.2.4 Evaluation of I_c

Based on the Biot-Savart law for one dimensional, thin strand current distributions

$$\vec{B}(\vec{r}) = \frac{\mu_0}{4\pi} I \int \frac{d\vec{s} \times \hat{r}}{|\vec{r} - \vec{r}'|^2}, \quad (4.3)$$

we can recalculate the current flow by solving the linear equation system

$$B_i = \frac{\mu_0}{2\pi} \cdot \sum_{j=0}^N \frac{(z_i - z'_j) \cdot I_j}{(y_i - y'_j)^2 + (z_i - z'_j)^2}. \quad (4.4)$$

At a position r_i , the magnetic field B_i , measured with the Hall probe i , is the superposition of all magnetic fields B_{ij} , caused by the currents I_j flowing at r'_j , with $\vec{r}_i = i \cdot \Delta z \cdot \hat{e}_z$, $\vec{r}'_j = \Delta y \cdot \hat{e}_y + (j - \frac{1}{2}) \cdot \Delta z \cdot \hat{e}_z$ and Δy as distance between the sample surface and the Hall probes and Δz as distance between the active area of two Hall probes.

5 Results

In the following chapter I will discuss the results of some tape measurements. Table 5.2 at the end of this chapter will give a brief overview of all our results.

5.1 M3-747

After several tests on short samples, we first used the Hall probe technique to analyze the tape M3-747 in full length of 116 m. We found very good correlation between the critical current and the remanent magnetization profile. The results are shown in figure 5.1. The I_c consists of a superposition of long and short fluctuations. The inset shows the short fluctuations with a length of ≈ 28 cm. These fluctuations are already observed in previous measurements and are found to correlate to width variations of the tape, which are very likely caused by the slitting process. The diameter of the disk knife is 28 cm. Two small dropouts at 5600 m and 5700 m are observed in the I_c measurements as well as with the Hall probes, but they are shifted in position by 22.9 cm, caused by uncertainties in measuring the position. The large dropouts at ≈ 77 m, 93 m, 103 m, 111 m and 113 m are not observed with the Hall probes and might be caused by a bad contact. On the other hand, the drops to 38.1 A at 30.9 m and to 37.8 A at 55.9 m are seen in both independent measurements. These bad spots are real.

The green and the magenta line indicate linear fits of the two measurements. The mean I_c of this tape is 48.80 A with a standard deviation of 2.36 A. The local I_c average is slightly decreasing over length with 9.21 mA/m. The Hall signal decreases too, but faster with 14.29 μ T/m. Therefore it is not possible to calibrate the Hall measurement only at the beginning of the tape. The local calibration factor is $c(x) = 4.01 + \frac{4x}{1000}$ A/mT, x is the actual position in meter. The average of the measured field is 19.12 mT with a standard derivation of 0.73 mT. We can further compare the ratio of the standard derivation and the average of the magnetization and the critical current measurement, which is 0.038 and 0.046, respectively.

In figure 5.2 the current distribution of this tape is shown. The currents are normally distributed (Gaussian distribution). The width of each box is 0.4 A.

5.2 M4-52

The following tape which was measured in full length was M4-52 from Superpower. This tape is also used for a superconducting magnet project at the National High Magnetic Field Laboratories. The knowledge of the I_c profile of the tape is crucial to improve the analysis of the quench behavior of the magnet. Several pairs of voltage tabs were fixed

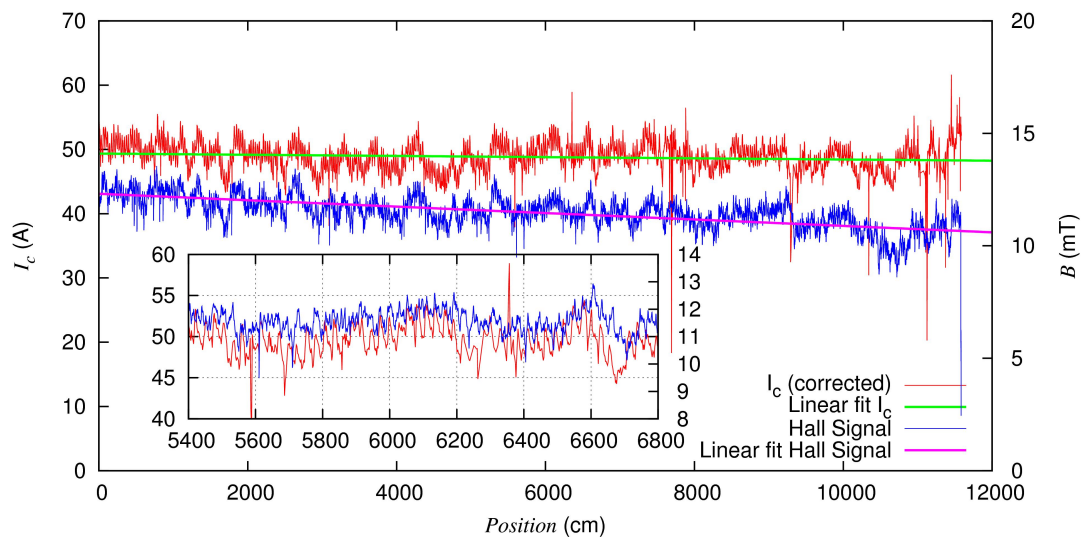


Figure 5.1: M3-747: Comparison of two measurement methods over nearly 120 m; the I_c and magnetization data correlate very well

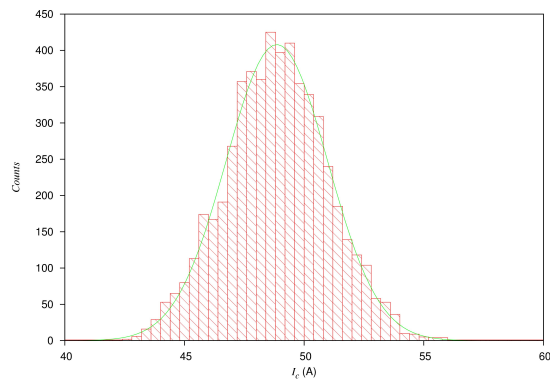


Figure 5.2: M3-747: Current distribution in the tape, a Gaussian function describes it very well

to the tape during the winding process. With the provided data, shown in figure 5.3, they were able to control special regions by measuring the voltage drop, where a quench is more probable during a test. The development of the I_c is not as clear as in the tape M3-747. The linear fits of the data are split in two parts ($<$ and $>$ 65 m). Below 65 m the critical current is slightly increasing. The same behavior was measured by the Hall probes. The signal is increasing with a similar slope. In the second part the mean I_c is strongly decreasing with increasing deviations. The Hall signal decreases as well, but much slower. The inset of fig. 5.3 shows the development of the standard deviation of the transport current measurement. The error bar in x direction indicates the region over which it was determined. In the Hall measurement one bad spot occurs at 57.5 m and was spotted with two different Hall sensors. It drops to 70 % of the average of its closest neighbors. If this drop is real it could have been damaged, while the tape was spooled back to the beginning between the I_c and magnetization measurement. Since it was not observed in the I_c measurement, it could be an artefact on the surface of the tape as well. For safety reason a voltage tab is recommended in this section of the tape during magnet tests.

	Mean I_c (A)	Standard deviation (A)	Standard deviation/Mean
Full length (113 m)	45.4	3.046	0.067
1st half (56.5 m)	47.1	1.686	0.036
2nd half (56.5 m)	44.0	3.178	0.072

Table 5.1: Results for the I_c measurement of tape M4-52; tape quality decreases with length

To compare the quality of the above-mentioned tape with M3-747, we can look at the ratio of the standard deviation and the mean value. A small number that implies a high mean I_c with small variations is desirable. Over the full length the ratio is 0.067, compared to M3-747 with 0.046 it is almost 50 % higher. However, the ratio for the first half is only 0.036 (see table 5.1). This shows that further improvements in the production process are necessary to ensure better quality of the superconducting layer over the full length.

5.3 M3-998 Insulated Tape

The 68 m long tape M3-998 was entirely insulated with polyester shrink tubes in the in-house superconducting insulation system for its use in superconducting coils. The magnetization measurements are contactless and therefore allow us to analyze insulated tapes as well. This feature is very interesting for the further development of heat treating insulation methods. By measuring the tape twice, before and after insulation, problems of this process can be determined and risks of damaging the tape can be avoided. In contrast, transport current measurements are not possible on insulated tapes.

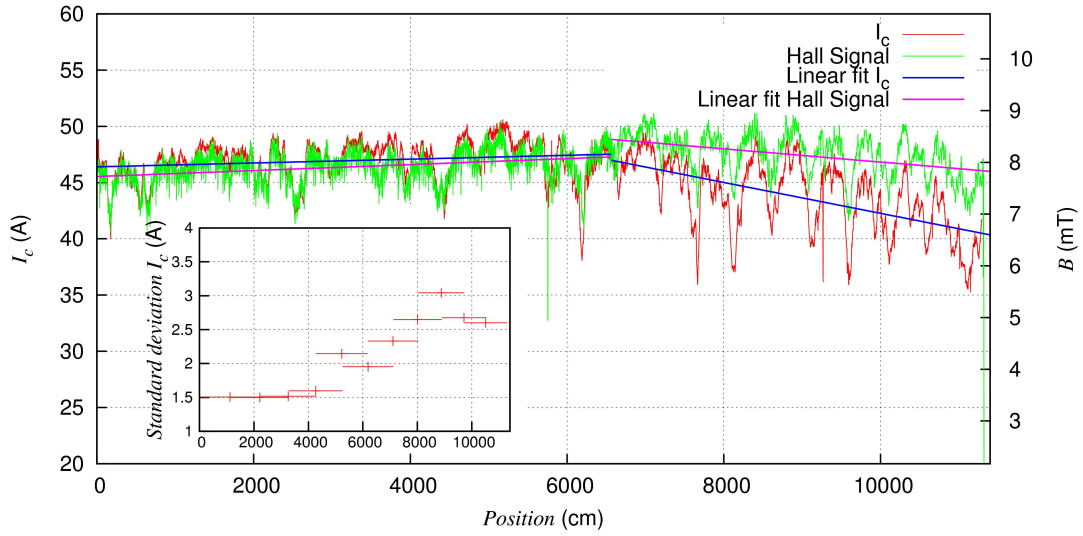


Figure 5.3: Results of I_c and Hall probe measurement of tape M4-52, with linear fits for two sections each ($<$ and $>$ 65 m); the inset shows the standard deviation of the I_c measurement for several regions

For the first time we used the sensor head with seven Hall probes during this measurement. A much higher resolution in tape width was achieved. The mean field is 8.18 mT with a very good ratio of standard deviation to mean value of 0.033. The tape itself cannot be measured absolutely by transport measurements due to its insulation. For this reason we soldered a collection of several short samples with different I_c values which are not insulated to the beginning of the M3 tape. By measuring both the I_c of those short tapes and the magnetization profile, the Hall probe scan can be calibrated in situ. By this method the mean in-field I_c of this tape results to 56 A, corresponding to a calibration factor of 6.86 A/mT.

Figure 5.4 shows five meters in detail. Variations in width are observed. This tape is a middle slit (MS), therefore both sides are cut and not straight. Those variations cause the 28 cm fluctuations in the I_c and magnetization curves. With seven Hall probes across the width of the tape, a field gradient can be calculated. Using equation 4.2 with $n = 4$, $z_{i+1} - z_i = 0.6$ mm we calculated the slope for the upper edge (m_u , HP a - HP d) and the lower edge (m_l , HP d - HP g). We showed in measurements described above that the field in the center of the tape is proportional to the critical current. The slopes m_u and m_l can now be compared to the central field profile (fig. 5.4 (a)). It is obvious that the slopes are proportional to the remanent magnetization and therefore to the critical current profile. The mean values for m_u and m_l are 5.8 mT/mm and 5.5 mT/mm, respectively. Hence, the expected field in the center is about 10 mT, which matches with the results, given that Hall probe d is not perfectly centered.

To calculate the current flow, equation 4.4 was used with $\Delta z = 0.6$ mm. The distance between tape and Hall probes Δy is crucial for this calculation. We calculated the current

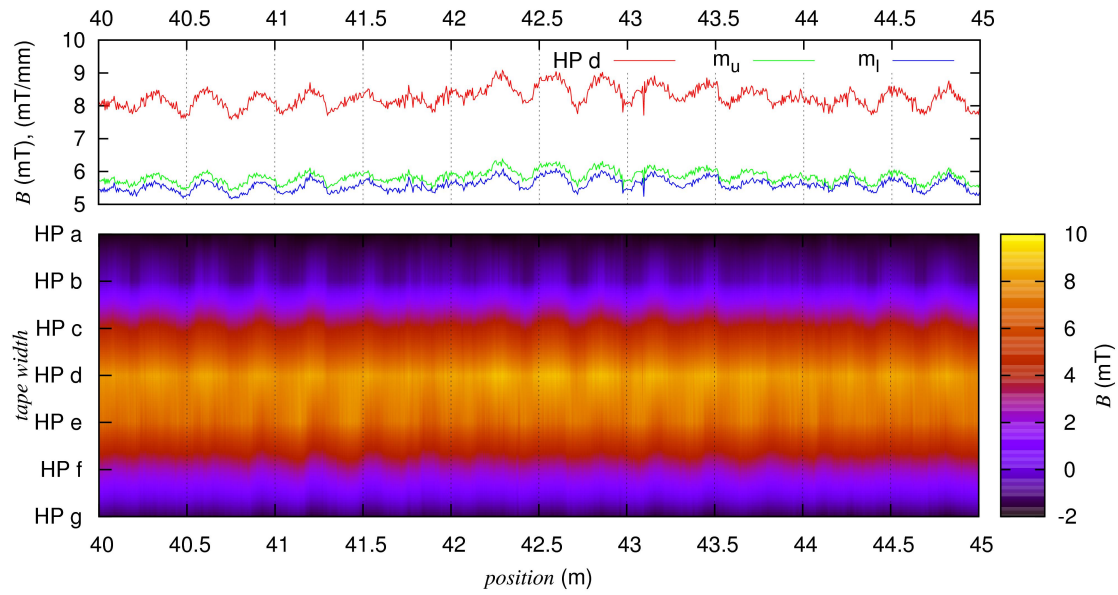


Figure 5.4: M3-998 in detail: (a) Field over the center of the tape (red curve), additional the upper and lower slope (green and blue) in mT/mm (b) 2d field map $B(x, z)$ (interpolated)

I with four different values for Δy : 0.5 mm, 0.7 mm, 1 mm and 1.2 mm. The results for a short section of five meters are compared in figure 5.5. An actual distance between 1 mm and 1.2 mm is most likely. Positive currents flow in positive x-direction. In fig. 5.5 (a) and (b) the 28 cm variations are not apparent and do not strongly influence the maximums of the current flow. On the other hand they are significant in fig. 5.5 (c) and (d).

Figure 5.6 shows the field and current profiles at $x=27.654$ m, interpolated by cubic splines. To show a more exact Bean like behavior, the resolution across the tape width is still not sufficient. But two linear fits in figure 5.6 (a) (green lines) indicate this Bean shape and the position of the center of the tape as well (line-line intersection). When mounting the Hall probe array, the center of the tape was missed by about 0.2 mm. Figure 5.6 (b) shows approximately the expected current distribution with currents flowing in positive and negative x-direction on the upper and lower edge, respectively. The current profile shown is calculated with $\Delta y = 1$ mm. It is clear that this profile is only a very simple approximation not regarding any boundary effects. Since there are only seven measured points across the width no corrections are made, e.g. that currents vanish at the edges.

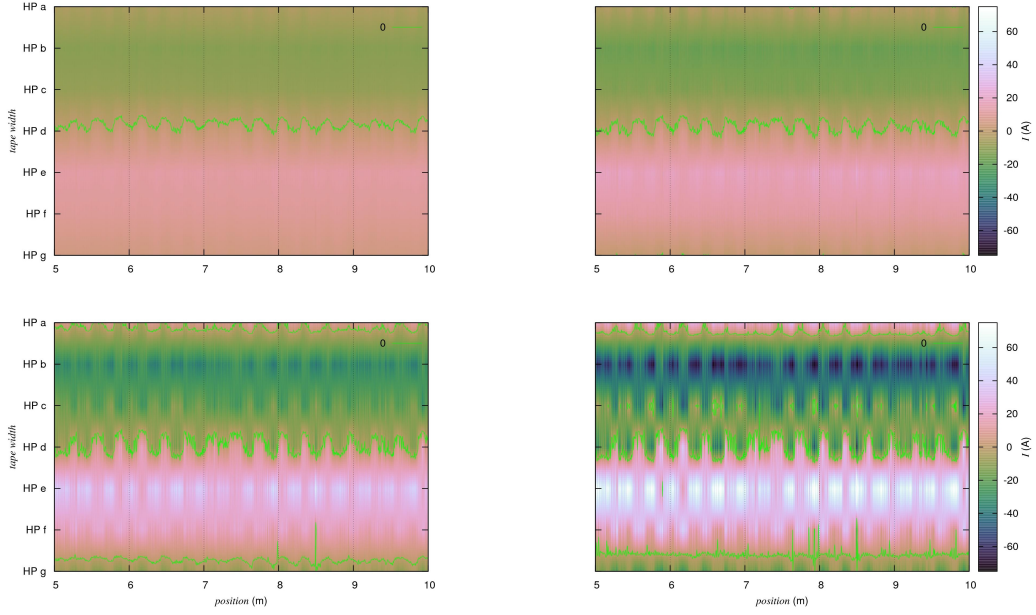


Figure 5.5: M3-998: 2d maps of current calculations $I(x, z)$ for different distances Δy between Hall probe surface and tape, (a) $\Delta y = 0.5$ mm, (b) $\Delta y = 0.7$ mm, (c) $\Delta y = 1$ mm, (d) $\Delta y = 1.2$ mm; the green lines indicate 0 A

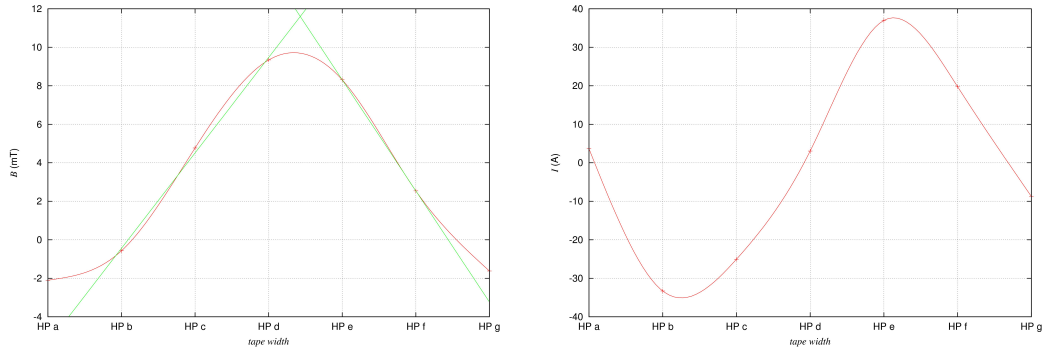


Figure 5.6: M3-998: Profile curves at position 27.7 m over tape width, consecutive points connected by natural cubic splines after rendering the data monotonic for (a) the measured field (b) the calculated current; the green lines in panel (a) are linear fits through points of HP b - HP d for the left side and HP e and HP f for the right

5.4 SP57

This tape was one of three used to wind an all superconducting magnet which has quenched. Quenches occur, if the field inside the magnet or the rate of change of the field is too large. Especially for coated conductors local defects can be a source of quenches. After the quench the tapes were unwind and analyzed with YatesStar. Indeed, after 37 m we found a huge drop to less than 50 % of the average I_c of this tape. Since the speed-up function was enabled, a rerun was necessary to resolve this defect in detail.

The mean I_c values for Channel one and two are 40.2 A and 38.98 A, with standard deviation to mean value ratios of 0.044 and 0.047, respectively. The average decreases with 4.5 mA/m. The self field I_c of the bad spot is about 13.9 A, in field it further drops to 5.4 A. The whole measurement is shown in figure 5.7. The inset of this figure shows all lines drop. The drops of the I_c measurements are wider. Usually the region in the center of the field defines the I_c , the distance between the voltage tabs can be neglected. In this case, the self field I_c of the damaged area is even worse than the average in-field I_c . Both I_c curves drop to the self field I_c of the bad spot as soon as it is in between the voltage tabs. When the defect moves into the center of the magnet, the critical current drops further. The Hall probe signal even drops to 0 mT. Over the full length the 28 cm fluctuations are again clearly perceptible.

For further investigations of this defect, a short sample of 20 cm was cut out of the tape with the defect in the center. This short sample fits into the magnetoscan setup at the Atominstitut in Vienna, where it was analyzed again. The sample was fixed in a dewar immersed in liquid nitrogen. A magnet, with a maximum field of 400 mT, was moved along the surface of the tape for magnetization purposes. After that a single Hall probe, fixed to a computer controlled stepper motor, scanned the tape surface with a step size of 0.5 mm. The scan is plotted in figure 5.8. The width of the defect is 21 mm. The apparently larger width (5-6 cm) of the defect in the I_c measurement is to due the finite distance between the voltage tabs as explained above.

These results proof the need of quality control of coated conductors for any applications and the validity of our methods. We were able to find a major defect, which caused the quench of the magnet. Further, mechanical handling, like winding and unwinding the tape does not necessarily harm the tape. We highly recommend to provide us with tapes before using them. Preliminary investigations should be established as standard procedure at the NHMFL, which could save working hours and Helium and prevent a possible damage of other tapes in case of a quench.

5.5 SP59

The results of the I_c and remanent field scans are shown in figure 5.9 (a). This tape has a high average critical current of 43.4 A with a root mean square deviation of 3.29 A. The ratio of those two values is 0.079. The average I_c decreases with 243 mA/m, calculated over the full length of the tape. The average of the field is 5.96 mT and its ratio with the standard deviation 0.061. It decreases with 12 μ T/m. In percent the critical current

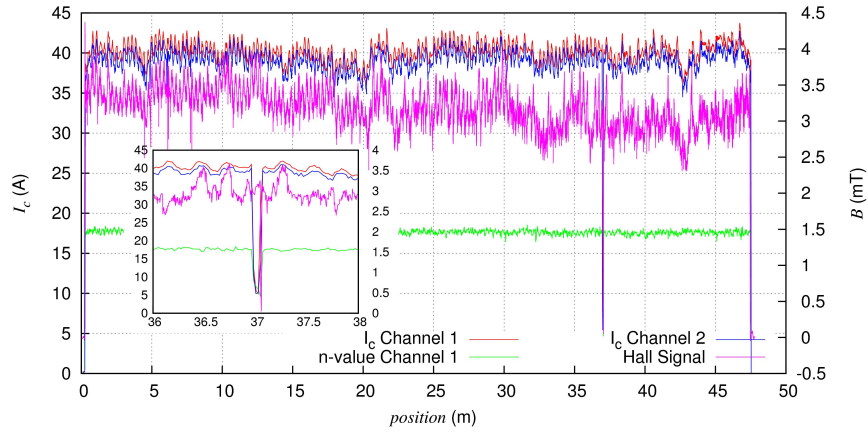


Figure 5.7: SP57: The results of the tape analysis; obvious defect at 37m, observed in all scans (both I_c channels and Hall probes) and in the n-value evaluation; the inset shows the defect in detail, the I_c drops to one eighth of the average

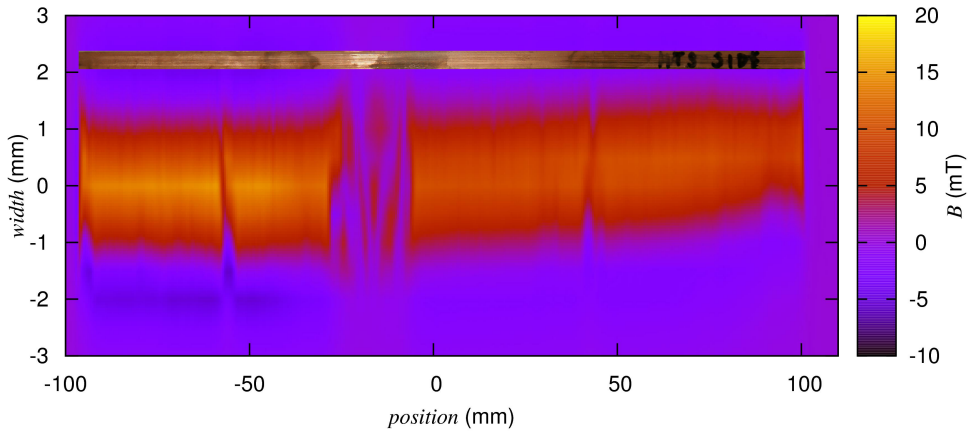


Figure 5.8: 2d map of the remanent field of the short sample cut out of the middle of SP57 to analyze the defect structure with a higher resolution; the defect is about 21 mm wide; a picture of the sample is overlapped to show no damages on the surface cause the vanishing of superconductivity (ratio of length to width is changed)

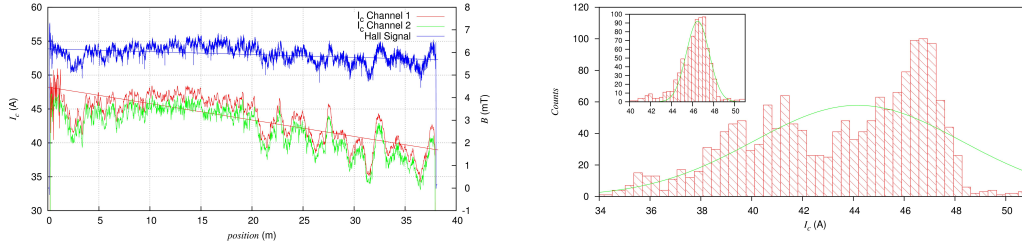


Figure 5.9: SP59: (a) The critical current and remanent field profile, with linear fits for the I_c of channel one and the Hall signal (central Hall probe); short and long fluctuations are observed; the variations in the first meter of the red line do not correlate to real I_c variations; (b) distribution of critical currents over full length (inset: only over first 20 m) of the coated conductor; a Gaussian distribution is fitted to the data

decreases with 0.6 % and the remanent field only with 0.2 %, indicated by the red and blue line in fig. 5.9 (a). The difference in the rates of change leads to a non-constant calibration factor, which results to $c(x) = 7.7 - \frac{x}{50}$ A/mT with x in meters. Several fluctuations superpose. Especially after 20 m the behavior of the critical current changes dramatically. Those long fluctuations seriously worsen the result of this tape. It remains unclear, if chemical or mechanical modifications of the production during the manufacturing process caused these fluctuations. The high amplitude of the red curve in the first meter might be caused by a bad contact. Similar signal variations are not observed in the signal of channel two nor the Hall measurement. Figure 5.9 (b) shows a histogram of the distribution of the currents. The inset takes only the first 20 m into account. A Gaussian function is fitted to the data. For the first half of the tape (inset) a Gaussian distribution approximately matches the current distribution while the full tape cannot be described by a Gaussian function. This distribution cannot be due to random processes during manufacturing.

5.6 Tape Collection (SP60-SP64)

The tape collection is a composition of ten short tape samples, which are soldered together. The 60 cm long samples were cut from both ends of the tapes SP60 - SP64, respectively. The terms inner (i) and outer (o) end relate to the orientation of the tapes in a spool, which was built using those tapes. Before the short samples got coupled together, their self field I_c at 77 K was measured by Dmytro Abramov at the NHMFL. In YatesStar we analyzed the in-field I_c and remanent field. The results are shown in figure 5.10 (a). There are three y-axes. The very left shows the range of the self field measurement which are pictured as red boxes, followed by the y-axis for in-field results. The label for the magnetic measurement is on the right side of the plot. The self field I_c was measured over 60 cm and, therefore is defined by the minimum critical current. The high green peaks of the signal of the central Hall probe (HP d) correspond to the coupling

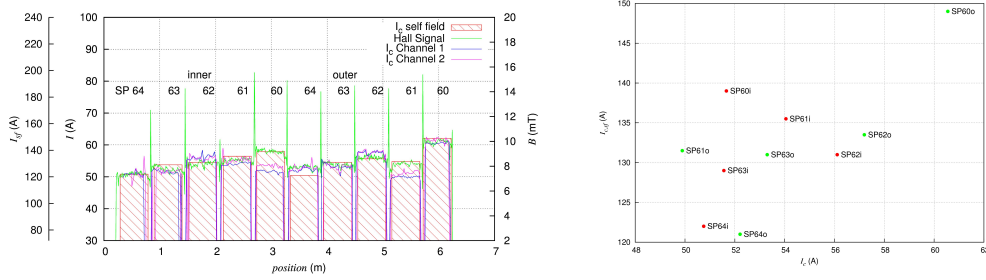


Figure 5.10: (a) Overlap of three different measurements of the 10 short samples of the tape collection: the red boxes are the results of the self field measurements with the scale on the very left, the green curve is the reel-to-reel Hall probe result and the blue and magenta profiles are in-field I_c values measured with YatesStar; (b) $I_{c,sf}$ over I_c , no simple correlation is observed, which is valid for all tapes; only for individual tapes higher $I_{c,sf}$ values correlate with higher in-field currents, with exception of SP64

joints between the tapes. The Hall Signal $B(x)$ and the self field critical current $I_{c,sf}$ correlate very well, which is obvious in the samples SP60i and SP61o, with exception of sample SP64o. The results are pictured again in figure 5.10 (b), where the self field critical current is plotted over the in-field critical current. The inner ends are indicated with red points, the outer with green ones. There is no simple correlation valid for all tapes. While viewing the tapes individually, a higher self field I_c correlates with a higher in-field current, with exception of tape SP64.

5.7 SP41

SP41 is a short tape with a low I_c . It is only used for tests of our measuring system, to find problems in our setup and improve the measurements. During one of the first tests in liquid helium, the first 10 m of the tape got destroyed, when it lost tension and got caught between a pulley and the extension. Subsequently added stabilizers ensure better measurements. For our testing procedures the destroyed areas in the tape were useful, by allowing us to adjust several measurements. Figure 5.11 compares unique reel-to-reel results at 4.2 K with transport current and magnetization measurements at 77 K. The remanent magnetization was produced by a magnetic field of 0.5 T, respectively. The remanent field at 4.2 K exceeds the magnetization at 77 K by a factor of 15. The self field critical currents at low temperatures are far beyond 1 kA. Correlations between the I_c curve and the green magnetization profile are obvious. The low temperature Hall probe measurement correlates to the critical current as well.

With the new developed measuring techniques further investigations on the influence of various defects, high and low fields, field sweeps and insulation methods over a wide temperature range can be done.

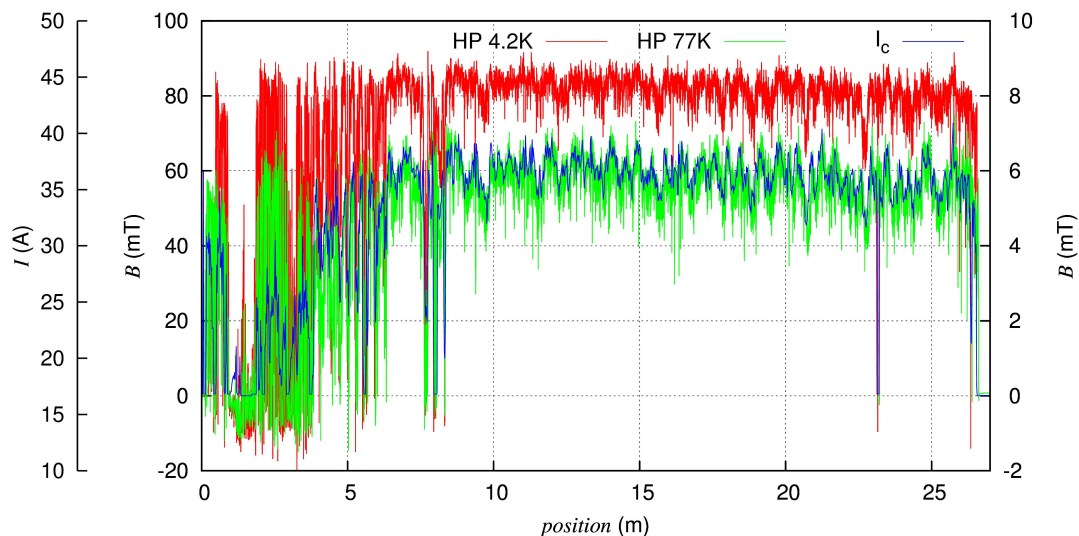


Figure 5.11: Comparison of reel-to-reel measurements at 4.2 K and 77 K; the very left scale corresponds to the I_c measurement at 77 K, and the right scale to the Hall probe measurement at 77 K

Superpower Label	In House Label	Project	Length (m)	\bar{I}_c (A)	R_{I_c}	R_B
M3-747-2-BS			116	48.8	46	38
M4-52-2-FS			110	45.4	67	109
M3-891-1 FS	SP41	YS* tests	26	29.6	75	43
M3-998-2 MS 1224.6-1324.6			69			33
M3-842-1 MS	SP53	32 T	54	37.4	32	76
M4-52-2 BS	SP57	32 T	48	40.2	44	87
M4-52-2 FS	SP59	32 T	38	43.4	79	61
M3-1029-1 MS 979-1089.7	SP60	32 T	1.2	56.2		
M3-1038-2 BS 148.44-258.44	SP61	32 T	1.2	52		
M3-1038-2 FS 423.44-533.44	SP62	32 T	1.2	56.7		
M3-1038-2 FS 309-419	SP63	32 T	1.2	52.5		
M3-1038-2 FS 419-529	SP64	32 T	1.2	51.5		

Table 5.2: Listing and labeling of measured tapes with results for 77 K measurements; R_{I_c} and R_B are the ratios of standard deviation to mean value multiplied by 1000 for the I_c and Hall probe measurements

6 Conclusions

The main results of this work were

- development of characterization of emerging superconductors for power generation/transmission and scientific and medical applications,
- quality testing for all superconducting high field magnets currently under construction at the NHMFL,
- detailed comparison of two characterization methods,
- discovery of problems in manufacturing process of CCs causing variations in quality,
- pioneer development of reel-to-reel measurements in liquid helium and
- two publications, currently in preparation and several conference presentations.

Bibliography

- [1] BEAN, C. P.: Magnetization of Hard Superconductors. In: *Phys. Rev. Letters* (1962)
- [2] BEAN, C. P.: Magnetization of High-Field Superconductors. In: *Rev. Mod. Phys.* (1964)
- [3] BRACCINI, V. ; XU, A. ; JAROSZYNSKI, J. ; XIN, Y. ; LARBALESTIER, D. C. ; CHEN, Y. ; CAROTA, G. ; DACKOW, J. ; KESGIN, I. ; YAO, Y. ; GUEVARA, A. ; SHI, T. ; SELVAMANICKAM, V.: Properties of recent IBAD–MOCVD coated conductors relevant to their high field, low temperature magnet use. In: *SUST* (2011)
- [4] BRANDT, E. H. ; INDENBOM, Mikhail: Type-II-superconductor strip with current in a perpendicular magnetic field. In: *Phys. Rev. B* 48 (1993), Nr. 17
- [5] COULTER, J. Y. ; HAENISCH, J. ; WILLIS, J. O. ; CIVALE, L. ; PIERCE, W. K.: Position and Magnetic Field Angle Dependent I_c for Long-Length Coated Conductors. In: *IEEE Transactions on Applied Superconductivity* 17 (2007), Nr. 2
- [6] COULTER, J. Y. ; HOLESINGER, T. G. ; KENNISON, J. A. ; WILLIS, J. O. ; RUPICH, M. W.: Nondestructive Investigation of Position Dependent I_c Variations in Multi-Meter Coated Conductors. In: *IEEE Transactions on Applied Superconductivity* 19 (2009), Nr. 3
- [7] FURTNER, S. ; NEMETSCHKE, R. ; SEMERAD, R. ; SIGL, G. ; PRUSSEIT, W.: Reel-to-reel critical current measurement of coated conductors. In: *SUST* (2004)
- [8] GRIMALDI, G. ; BAUER, M. ; KINDER, H.: Continuous reel-to-reel measurement of critical currents of coated conductors. In: *Applied Physics Letters* (2001)
- [9] HALL, E. H.: On a new Action of the Magnet on Electric Currents. In: *American Journal of Mathematics* 2 (1879)
- [10] INOUE, M. ; ABIRU, K. ; HONDA, Y. ; KISS, T. ; IJIMA, Y. ; KAKIMOTO, K. ; SAITOH, T. ; NAKAO, K. ; SHIOHARA, Yuh: Observation of Current Distribution in High T_c Superconducting Tape Using Scanning Hall-Probe Microscope. In: *IEEE Transactions on Applied Superconductivity* (2009)
- [11] JAROSZYNSKI, J. ; ABRAIMOV, D. ; BRACCINI, V. ; SANTOS, M. ; XU, A. ; POLYANSKII, A. ; COULTER, Y. ; SINCLAIR, J. W. ; WEIJERS, H. ; MARKIEWICZ, W. D. ; LARBALESTIER, D.C.: Testing procedures on IBAD-MOCVD coated conductors for thier use at high magnetic field and low temperature in magnet applications.

- [12] KIM, Y. B. ; HEMPSTEAD, C. F. ; STRNAD, A. R.: Magnetization and Critical Supercurrents. In: *Phys. Rev.* (1963)
- [13] THAKU, K. P. ; BADCOCK, R. A. ; LONG, N. J. ; HAMILTON, K. A.: Analysis of Remnant Field Detected by Hall Sensors. In: *Sensors, IEEE* (2009)
- [14] WEIJERS, H. W. ; MARKIEWICZ, W. D. ; LARBALESTIER, D. C.: Development of a 32 T All-Superconducting Magnet System using $\text{YBa}_2\text{Cu}_3\text{O}_{7-x}$ Coated Conductors / National High Magnetic Field Laboratory. 2012. – Forschungsbericht
- [15] WILLIS, J. O. ; COULTER, J. Y. ; RUPICH, M. W.: n-Value Analysis of Position-Dependent Property Variability in Long-Length Coated Conductors. In: *IEEE Transactions on Applied Superconductivity* 21 (2011), Nr. 3
- [16] XU, A. ; BRACCINI, V. ; JAROSZYNSKI, J. ; XIN, Y. ; LARBALESTIER, D. C.: Role of weak uncorrelated pinning introduced by BaZrO_3 nanorods at low-temperature in $(\text{Y,Gd})\text{Ba}_2\text{Cu}_3\text{O}_x$ thin films. In: *Phys. Rev. B* 86 (2012)
- [17] ZEHETMAYER, M. ; FUGER, R. ; EISTERER, M. ; HENGSTBERGER, F. ; WEBER, H. W.: Assessment of the local supercurrent densities in long superconducting coated conductors. In: *Applied Physics Letters* 90 (2007), Nr. 3